THE ASTROPHYSICAL JOURNAL, 449:888–893, 1995 August 20

WFPC2 IMAGING OF THE CIRCUMSTELLAR NEBULOSITY OF HL TAURI[1]

KARL R. STAPELFELDT,[2,3] CHRISTOPHER J. BURROWS,[4] JOHN E. KRIST,[4] JOHN T. TRAUGER,[2] J. JEFF HESTER,[5] JON A. HOLTZMAN,[6] GILDA E. BALLESTER,[7] STEFANO CASERTANO,[4] JOHN T. CLARKE,[7] DAVID CRISP,[2] ROBIN W. EVANS,[2] JOHN S. GALLAGHER III,[8] RICHARD E. GRIFFITHS,[9] JOHN G. HOESSEL,[8] JEREMY R. MOULD,[10] PAUL A. SCOWEN,[5] ALAN M. WATSON,[6] AND JAMES A. WESTPHAL[11]

Received 1994 October 24; accepted 1995 March 7

ABSTRACT

Planetary camera images of HL Tauri have been obtained through *V*-, *R*-, and *I*-band filters using the Wide Field and Planetary Camera 2 aboard the refurbished *Hubble Space Telescope*. These images show that HL Tauri is entirely reflection nebulosity at optical wavelengths, with no optical star visible to a limiting magnitude of $V = 25.5$. The optical nebula extends northeast of the stellar position along the direction of HL Tau's optical jet and has an unusual C-shaped morphology. The bright core of the nebula is only 1″ in size and is centered only 1″.2 from the actual stellar position. We estimate that visual extinction toward the unseen point source is at least 22 mag and that the stellar photospheric luminosity must be at least 3 $L_\odot$. These findings corroborate other evidence that this star is significantly younger and more embedded than typical T Tauri stars.

Subject headings: circumstellar matter — stars: individual (HL Tauri) — stars: pre–main-sequence

1. INTRODUCTION

HL Tauri has been considered a prototype solar-mass T Tauri star with a circumstellar disk analogous to the early solar nebula prior to planet formation (Sargent 1989). Several properties of HL Tauri suggest that it is unusual among T Tauri stars. It is the source of a collimated optical jet at PA 51°. Strong blueshifted forbidden emission is superposed onto the stellar spectrum, indicating that the jet forms very close to the star (Mundt et al. 1990). HL Tau is also an exceptional object in terms of its circumstellar material properties. It has the highest optical polarization (11%) among the T Tauri stars surveyed by Bastien (1982). Infrared ice and silicate absorption features are present in its spectrum (Whittet et al. 1983; Cohen & Witteborn 1985). It is a strong *IRAS* source and one of the few T Tauri stars with a flat spectral energy distribution out to 100 μm (Adams, Lada, & Shu 1988). In the millimeter and submillimeter continuum, HL Tau is by far the brightest source among all the T Tauri stars in Taurus, with a circumstellar mass near 0.1 $M_\odot$ being indicated (Beckwith et al. 1990). Millimeter interferometer maps show a flattened distribution of ^{13}CO molecular emission extending to radii of 2000 AU (15″; Sargent & Beckwith 1991) with a velocity structure consistent with a combination of rotation and infall motion in a circumstellar disk (Hayashi, Ohashi, & Miyama 1993). Submillimeter and millimeter interferometry show that the densest part of the disk is much smaller (0″.7 = 100 AU in diameter: Lay et al. 1994; Sargent & Koerner 1995). A final distinguishing characteristic of HL Tau is that it is classified as a "continuum star"—the stellar spectrum shows only weak intermittent absorption features (Cohen & Kuhi 1979). This has been interpreted as strong veiling of the photospheric spectrum by continuum emission produced by accretion onto the central star (Basri & Batalha 1990). The combination of unusually prominent signatures of outflow, circumstellar matter, and accretion suggest that HL Tau is younger than typical T Tauri stars, and thus it may be one of the few optically visible protostellar objects.

High spatial resolution imaging of HL Tau at visible wavelengths is of great interest because it offers the opportunity to probe the distribution of matter and optical depth in the circumstellar disk and envelope. Spectral models predict that the disk should be opaque at visible wavelengths (cf. Beckwith et al. 1990), and thus only its outer surfaces should be illuminated. Models for the visible light scattered by such disks and associated envelopes have been calculated by Whitney & Hartmann (1992, 1993). Our *HST* observations were designed to study this circumstellar reflection nebulosity against the bright background of a stellar point-spread function.

2. OBSERVATIONS

Three images of HL Tau were obtained using the Wide Field and Planetary Camera 2 (WFPC2) aboard the *Hubble Space Telescope* (*HST*). The corrective optics of WFPC2 compensate for the spherical aberration present in *HST*'s primary mirror, yielding a point-spread function Airy disk with diameter of 0″.12 at $\lambda = 555$ nm. A review of the WFPC2 on-orbit status is given by Trauger et al. (1994). The HL Tau images were taken

[1] Based on observations with the NASA/ESA *Hubble Space Telescope*.

[2] Mail Stop 179–225, Jet Propulsion Laboratory, 4800 Oak Grove Drive, Pasadena, CA 91109.
[3] krs@wfpc2-mail.jpl.nasa.gov.
[4] Space Telescope Science Institute, 3700 San Martin Drive, Baltimore, MD 21218.
[5] Department of Physics and Astronomy, Arizona State University, Tyler Mall, Tempe, AZ 85287.
[6] Lowell Observatory, Mars Hill Road, Flagstaff, AZ 86001.
[7] Department of Atmospheric, Oceanic, and Space Sciences, University of Michigan, 2455 Hayward, Ann Arbor MI 48109.
[8] Department of Astronomy, University of Wisconsin, 475 North Charter Street, Madison, WI 53706.
[9] Department of Physics and Astronomy, Johns Hopkins University, Bloomberg 501, 3400 North Charles Street, Baltimore, MD 21218.
[10] Mount Stromlo and Siding Spring Observatories, Australian National University, Weston Creek Post Office, ACT 2611, Australia.
[11] Division of Geological and Planetary Sciences, Mail Stop 170–25 Caltech, Pasadena, CA 91125.

using the f/28.3 Planetary Camera (1 pixel = 0.″0455) on 1994 February 27 with the following filters and exposure times: F555W, 350 s; F675W, 120 s; and F814W, 60 s. Image-processing steps included subtraction of bias levels derived from rows 8–14 of the overscan, subtraction of a superbias image, subtraction of a composite dark frame scaled to the individual exposure times, the removal of cosmic rays via replacement of affected pixels by a local median, and flat-fielding. Photometric calibration of the images was done using data from version 2.0 of the WFPC2 Instrument Handbook (Burrows 1994). Astrometric calibration of these images was done using the solution given by Holtzman et al. (1995)

3. RESULTS

The most striking feature of these images is the complete absence of an optical stellar point source; only reflection nebulosity is present (Fig. 1 [Pl. 23] and Fig. 2*a*). The nebula seen by *HST* is just a few arcseconds across and thus must represent the bright inner core of the reflection nebula which extends beyond 10″ from HL Tau in all directions (Gledhill & Scarrott 1989). Most of the optical light comes from the central arcsecond^2, a fact which accounts for how the nebula was mistaken for the star itself in ground-based studies. This bright central region has an unusual C morphology, with the arms of the C pointing north. The southwestern edge of the nebula is sharp; other edges are much more diffuse.

The distribution of the $V-I$ (F555W − F814W) color in the nebula is shown in Figure 2*b*. As would be expected from ground-based photometry, the nebula has an overall red color. The brightest part of the nebula is also the least red ($V-I=1$ mag), with the bluest region found just north of the bright east-west bar which forms the back of the C. The greatest reddening is found on the faint southwest edge of the nebula, with $V-I=2.5$ mag at a spot in this region. The dark region forming the interior of the nebular C shows little color difference from its surroundings.

It is critically important to establish the stellar position of HL Tau with respect to the optical reflection nebula. The most precise stellar position available is given by Rodríguez et al. (1994) from VLA 3.6 cm radio continuum maps: $\alpha = 04^h28^m44^s.38$, $\delta = +18°07'35''.0$ with an uncertainty of 0.″1; this agrees well with the 1.3 mm continuum position determined by Sargent & Koerner (1995). Unfortunately, only one guide star is visible to the *HST* Fine Guidance Sensors when observing HL Tau, and thus it was not possible to determine a good position for the optical nebula from our observations. Herbig & Bell (1988) and Strom et al. (1986) give absolute optical positions for HL Tau which, although disagreeing by a full arcsecond, both place the nebula northeast of the radio position by more than 1″.

The only satisfactory way to locate the star in the *HST* frames is to assume that the VLA radio continuum source is spatially coincident with the star itself and to use the nearby star XZ Tau as a reference point. XZ Tau lies about 24″ east of HL Tau and is also detected at 3.6 cm by Rodríguez et al. Using the offset between the VLA positions of these two stars, it should be possible to determine the radio position of HL Tau in the *HST* images to within 0.″2. Unfortunately XZ Tau itself does not appear on our PC image; it falls just off the top right-hand corner of the PC detector and thus is not imaged by any of the WF cameras. We can still proceed without knowledge of XZ Tau's position by using it as a reference point for offset astrometry. The vector between the HL Tau radio source and the optical nebula is simply equal to the difference between the XZ Tau/HL Tau radio offset vector and the XZ Tau/HL Tau optical offset vector. The radio offset vector is $\Delta\alpha = -23''.9$, $\Delta\delta = +0''.5$. Optical offset vectors derived from Herbig & Bell (1988) ($\Delta\alpha = -22''.5$, $\Delta\delta = +1''.0$) and Strom et al. (1986) ($\Delta\alpha = -22''.8$, $\Delta\delta = +1''.0$) disagree by 0.″3. In hopes of resolving this discrepancy, we have measured the offset between HL Tau and XZ Tau using V-band CCD images obtained at the Lowell Observatory Hall Telescope in 1994 March. After solving for the plate scale and rotation in this

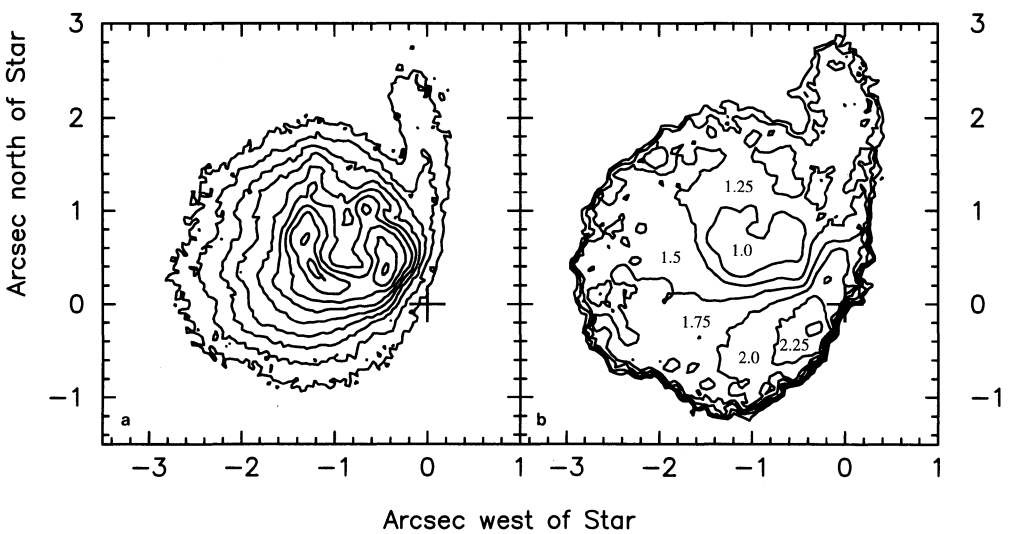

FIG. 2.—(*a*) A contour map of the WFPC2 F555W image of HL Tau. The highest contour level corresponds to a surface brightness of 14.7 mag arcsec^{-2}, the lowest corresponds to 18.7 mag arcsec^{-2}, and the contour interval is 0.5 mag arcsec^{-2}. (*b*) A contour map of the F555W − F814W color distribution in the HL Tau reflection nebula (essentially equivalent to the $V-I$ color). The contour interval is 0.25 mag. The data have been smoothed over a 3 × 3 pixel box, and the color map has been truncated to include only regions of good signal-to-noise ratio.

Young Star HL Tauri

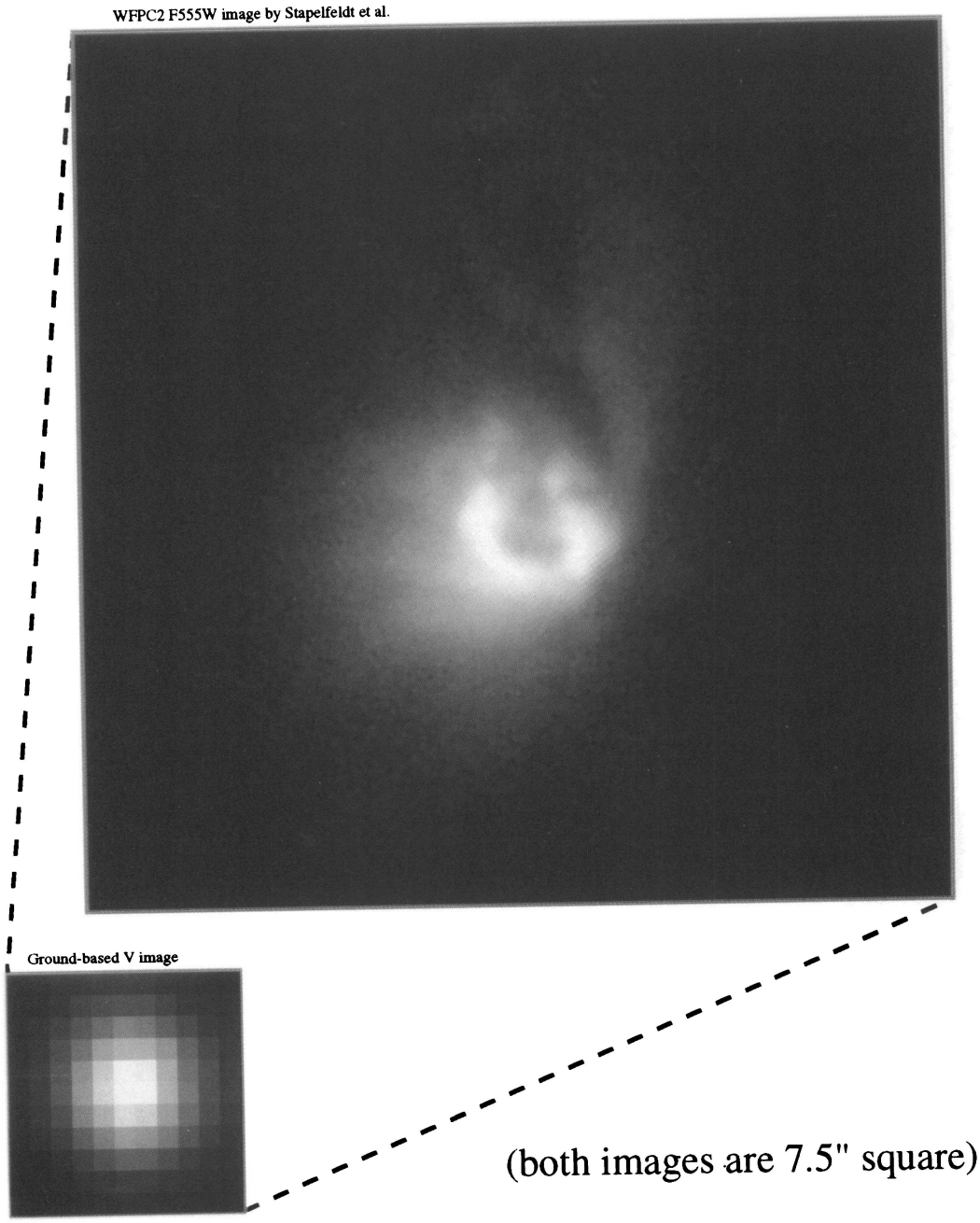

FIG. 1.—A logarithmic gray-scale depiction of the WFPC2 F555W image of HL Tau, compared to a ground-based *V* image taken with 2″ seeing. Both images are 7″.5 square. North is up, and east is to the left.

STAPELFELDT et al. (see 449, 889)

direct imaging system using an astrometric field in M67 (Montgomery, Marschall, & Janes 1993), we find an optical offset vector of $\Delta\alpha = -23''.0$, $\Delta\delta = +0''.7$, with an uncertainty $0''.2$; this result does not agree with either of the published offsets. Thus the available ground-based astrometry can only constrain the centroid of the optical nebula to lie generally northeast of the VLA postion at a distance between $0''.9$ and $1''.4$. This rules out the possibility that the star could lie within the bright nebulosity.

Although XZ Tau does not appear in our images, it does lie close enough to the edge of the Planetary Camera image so that sharp diffraction spikes can be seen. XZ Tau is a close binary (Haas, Leinert, & Zinnecker 1990), and the spikes at PA 99° are clearly doubled with a separation of $0''.3$. It is not yet clear which optical component corresponds to the unresolved XZ Tau VLA source, so we adopt the center of the system as a compromise reference point. The intersection of the perpendicular diffraction spikes defines the "virtual" pixel position for the center of the XZ Tau system: $x = 768$, $y = 822$. Using the offset between the HL Tau and XZ Tau radio sources reported by Rodríguez et al. and carefully accounting for the effects of WFPC2's field distortion on the offset astrometry, we derive $x = 463$, $y = 385$ as the pixel position for the star. This places the entire nebula on the northeast side of HL Tau, with the centroid of the scattered light offset by $1''.2$ at PA = 59°. There is very little nebular light at the inferred stellar position.

The position determined for the star is quite reasonable in light of what is known about other young stellar object reflection nebulae. First, the star is located on the side of the nebula opposite to the blueshifted optical jet—that is, "upstream" of the nebula as would be expected. Second, the star is found on the side of the nebula which has the most sharply defined edge (see Fig. 2*a*). The concentration of circumstellar matter at the central object should lead to larger absorbing columns and thus steeper gradients in nebular light as the stellar position is approached, just as we observe for HL Tau. Our determination of the stellar position is also corroborated by Beckwith & Birk (1995), who find that the centroid of the HL Tau light shifts to the northeast between *K* band and *J* band.

To establish limiting magnitudes for HL Tau itself, Planetary Camera point-spread functions of various amplitudes were added into the images at the radio position established above. For each image a scaling level for the PSF was determined, below which a PSF became indistinguishable by eye against the background emission. The results lead to the following limiting magnitudes: $V > 25.5$, $R > 24.0$, and $I > 22.9$. The I limit reflects the measured brightness of the red spot in Figure 2*b*, which is 0.3 mag brighter than our sensitivity limit. These limits are nearly 10 mag fainter than the reflection nebula itself at all three wavelengths.

4. DISCUSSION

It is not entirely surprising that we have found HL Tau to be an embedded young stellar object. One major clue is the star's large optical polarization of 11%; in their modeling of the scattering envelopes of young stellar objects, Whitney & Hartmann (1992, 1993) found that it was very difficult to obtain such a large polarization without obscuring the central star. Another clue is the presence of infrared ice and silicate absorptions in the star's spectrum, both of which argue for extinctions several times greater than those derived by fitting the star's optical spectrum (Cohen 1983). It is now apparent that optical and infrared light follow different paths to the observer and thus are affected by different amounts of extinction. Last, it had been believed that the ratio of infrared to optical luminosity for HL Tau was fairly large (7.0). Hamann & Persson (1992) have identified a group of such sources which includes HL Tau and suggested that their spectral energy distributions might be distorted by reflected light.

4.1. *Nebula Morphology*

At its bright core, the HL Tau reflection nebula appears significantly different from typical young stellar object reflection nebulae observed at arcsecond resolution. Rather than a smooth cometary nebula distributed symmetrically about the outflow axis, the inner core of the HL Tau nebula appears clumpy and lacks the outflow symmetry (Fig. 3 [Pl. 24]). Most of the nebular light originates in a C-shaped ridge of emission. On much larger scales a similar morphology is seen in the HH 83 reflection nebula (Reipurth 1989); however, in the case of HL Tau the jet axis does not trace through the open side of the C. It is unclear whether such unexpected subarcsecond structures are peculiar to HL Tau or whether they might also be revealed in other YSO reflection nebulae when imaged at *HST* resolution.

The only available ground-based image which approaches *HST* resolution is the $0''.4$ resolution *K*-band infrared speckle map of Beckwith et al. (1989). We have transformed this 2 μm image to a common size scale with the WFPC2 F555W image and aligned them by assuming a spatial coincidence between the infrared star and the 3.6 cm VLA source. The result is shown as a contour overlay in Figure 3. The star and southwest lobe of the 2 μm nebula are absent from the WFPC2 image because of the much larger extinction at 0.55 μm. There are two clear similarities in nebular structure between the two wavelengths. First, some of the brightest nebulosity extends eastward from the star as a narrow ridge of emission (the back of the optical C). The optical ridge is offset north of its infrared counterpart. Second, a faint arc of emission sweeps north from the stellar position; the optical arc is offset east of its infrared counterpart. These similar structures and their offsets with wavelength can be understood if the blueshifted outflow has cleared a cavity along the outflow axis. Along the walls of this cavity, the reflecting surface for optical light will appear interior to the the reflecting surface for infrared light (i.e., closer to the outflow axis) because optical photons penetrate a much smaller column of cavity wall material before being scattered. Thus the optical structures appear offset toward the outflow axis, as we observe.

It is unclear what gives rise to the C structure in the optical nebula; two possibilities are the distribution of absorbing material and the distribution of reflecting material. A foreground clump in the circumstellar envelope could superpose a dark blot on what might otherwise appear as a symmetric cometary nebula. Such a clump need not be very massive and is unlikely to be dynamically stable. The clump is absent at 2 μm, which for a standard reddening law suggests that A_V could be at most a few magnitudes. However, little or no reddening is observed in the dark interior of the C (Fig. 2*b*). As for reflecting material, the C could arise from either enhanced reflection at the bright regions (a special scattering geometry?) or diminished reflection in the interior of the C (lower column density of scatterers). A final possibility is that shadowing occurs along the nebula's line of sight to the stellar photosphere. Polariza-

PLATE 24

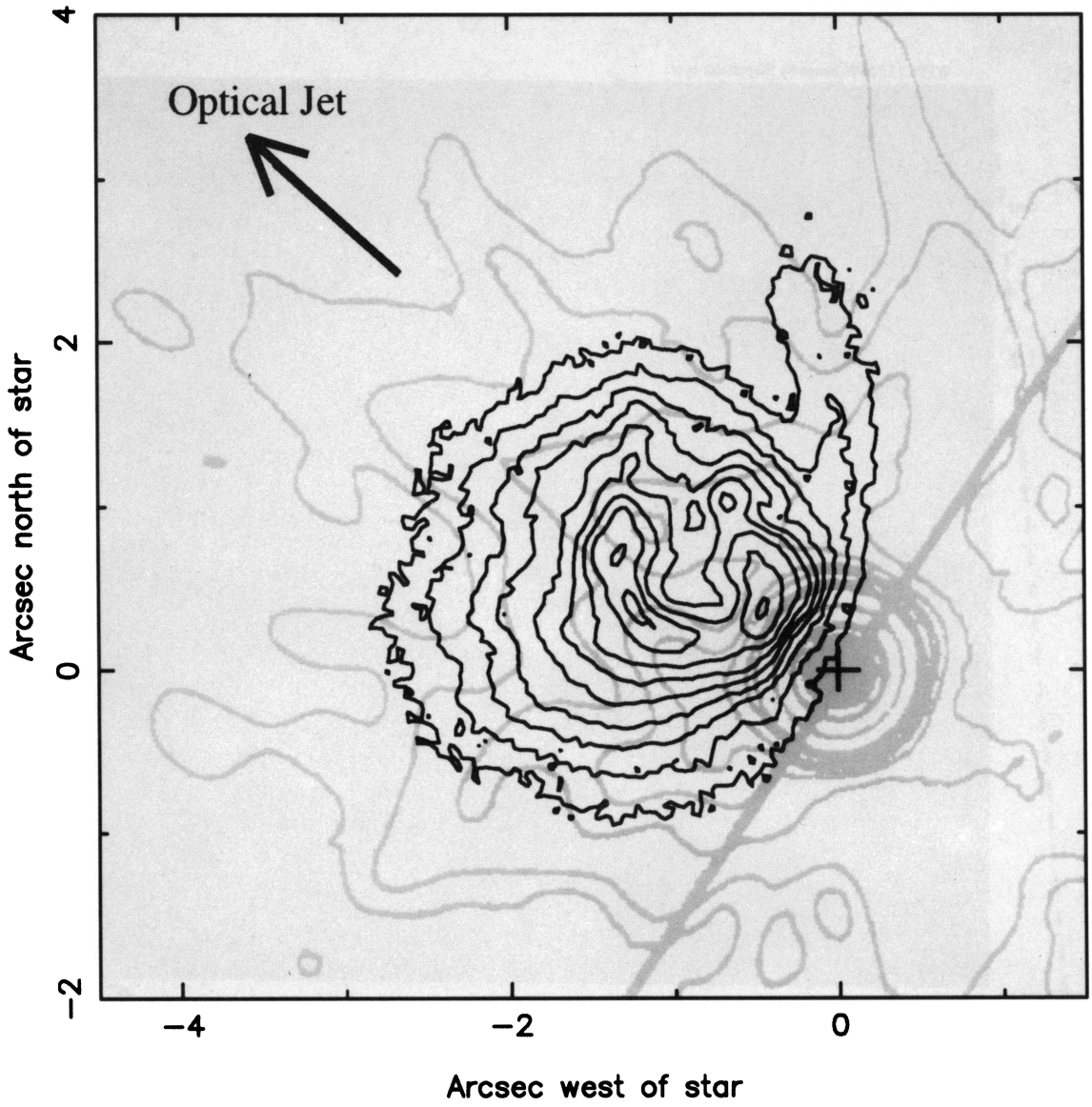

FIG. 3.—A contour map of the WFPC2 F555W image of HL Tau (*dark contours*) overlaid on the 2.2 μm contour map of Beckwith et al. (1989) (*gray contours*). In the *HST* image, the highest contour corresponds to a surface brightness of 14.7 mag arcsec^{-2}, the lowest corresponds to 18.7 mag arcsec^{-2}, and the contour interval is 0.5 mag arcsec^{-2}. Beckwith's gray bar running at PA = 146° indicates the plane of the disk seen in molecular gas.

STAPELFELDT et al. (see 449, 890)

tion imaging will help to discriminate among these scenarios. The northeast arm of the nebular C is bounded by the axis of the optical jet, which suggests that the outflow does play a role in defining the unusual shape of this nebula. It should be emphasized that the nebula is reasonably symmetric about the outflow axis at low surface brightness levels, and thus an illuminated outflow cavity remains the general framework for any model that explains the C morphology.

There is no direct evidence for HL Tau's circumstellar disk in our WFPC2 images. This is not really surprising because the disk is believed to be very optically thick at visual wavelengths, and thus starlight cannot penetrate its interior. However, the disk should truncate the optical reflection nebulosity in the region nearest the star; thus the disk orientation can be inferred from the position angle of the dense contours on the southwest side of the nebula. These contours follow PA 145°, which agrees closely with the direction of elongation of the larger scale ^{13}CO structure (Hayashi et al. 1993; Sargent & Beckwith 1991), of the arcsecond scale 1.3 mm continuum core (Sargent & Koerner 1995), and of the subarcsecond 870 μm continuum source (Lay et al. 1994). Rodríguez et al. have proposed a disk orientation near PA 90° on the basis of an eastward extension of 3.6 cm continuum emission in their VLA maps. Our *HST* observations do not support this and suggest instead that the radio extension could be tracing the same structure which gives rise to the east ridge of optical and near-IR nebulosity at the same location.

If the dense contours on the southwest edge of the nebula do trace obscuration by the circumstellar disk, then further inferences can be made about the formation of the cavity. The region where the nebular contours lie parallel to the disk plane extends over a linear distance of about 100 AU (0.″7); this should correspond to the diameter of the outflow cavity where it meets the disk plane. This diameter is essentially the same as the disk diameter measured at submillimeter and millimeter wavelengths (Lay et al. 1994; Sargent & Koerner 1995). This agreement is unlikely to be mere coincidence; instead, it suggests that a single physical process determines the size scale of both structures. This process could be infall, in which case the anisotropic collapse of a rotating cloud core produces the existing disk and leaves behind evacuated polar cavities (Boss 1987). Under this interpretation, the linear extent of parallel contours at the southwest edge of the nebula would correspond to the diameter of the centrifugally supported disk. Another possible explanation for the similar sizes of the disk and the base of the optical nebula could be a disk wind origin for an outflow which creates the cavity.

With the star seen only by reflected light, it is possible that the kinematics inferred from the radial velocities of optical spectral features may be distorted near the star. Optical emission lines from the jet could be anomalously blueshifted by reflection from stationary material along the jet axis. This effect has been observed in the form of high-velocity blue wings in the HH 1 jet by Solf & Böhm (1991). Similarly, redshifted 8800 Å C_2 absorption features observed by Grasdalen et al. (1989) could arise via infall of the reflecting clouds toward the star instead of infall along our line of sight to the nebula. Circumstellar kinematics derived from $\lambda < 1$ μm spectroscopy must be interpreted with caution.

4.2. *Stellar Characteristics of HL Tau*

Absorption features have occasionally been seen in the optical spectrum of HL Tau, and from these a stellar spectral type of K7 was estimated by Cohen & Kuhi (1979). Previous workers have assumed that the optical photometry of HL Tau corresponded to a reddened $T_{\rm eff} = 4000$ K photosphere and fitted the optical spectrum to derive the extinction and the stellar luminosity. Best prior estimates of these parameters were an extinction $A_V = 3$–7 mag and a luminosity of 1 $L_\odot$ (Beckwith et al. 1990; Adams, Emerson, & Fuller 1989). The optical invisibility of the star reported in this paper clearly indicates that these previous luminosity and extinction determinations must be revised and that a new assessment of HL Tau's stellar characteristics and evolutionary state is required.

Any study of HL Tau's spectral energy distribution must begin by identifying the contribution of the stellar photosphere. Unfortunately, it is now clear that no direct optical photometry of the star is available; there is only the brightness of the compact reflection nebula and limiting magnitudes at the stellar position. Thus it is not possible to derive directly a stellar luminosity and extinction without introducing outside assumptions. One simple approach is to use the photometry of the reflection nebula to infer the stellar magnitudes. The integrated nebula brightness reflects HL Tau's optical magnitude diminished by the extinction along the star-nebula-observer path and by the nebula's fractional solid angle as seen from the star. The opening angle of a cone whose vertex is at the stellar position and whose surface spans the fourth lowest contour in Figure 2*a* (surface brightness = 17.2 mag arcsec^{-2}) is about 90°, which when converted to a fractional solid angle means that the observed nebula intercepts no more than 15% of the optical light from the star. Assuming that the reflected light distributes isotropically and that ground-based extinction determinations are correct for the indirect path followed by light from the star, the nebular solid angle suggests that the true optical luminosity must be 6–7 times greater than previous ground-based estimates, or 6–7 $L_\odot$. This geometrical gain factor is dependent on the exact distance between the star and the nebula and thus must be considered uncertain by 30%. Additional uncertainty comes from the unusual nebula morphology, which suggests that some of the starlight emerging within the nebular cone might escape and not be observable via reflection.

A second approach for estimating the stellar luminosity is to extrapolate the stellar spectrum into the visible from near-infrared wavelengths and to integrate this to derive a luminosity. With the optical emission from the system dominated by reflected light and the infrared emission dominated by circumstellar matter, the near-infrared photometry offers the best opportunity to isolate photospheric fluxes. At 2.2 μm in particular, the speckle image of Beckwith et al. (1984, 1989) clearly shows a point source which contains 70% of the total 2.2 μm flux. The integrated K magnitude for HL Tau is 7.1 (Strom et al. 1989); the point source by itself thus corresponds to $K = 7.5$. However, this point source includes other sources of emission in addition to the stellar photosphere. At optical wavelengths the photospheric absorption spectra of the most active T Tauri stars appear washed out because of emission from a strong veiling continuum. This veiling is believed to represent energy released by accretion at the star/disk boundary layer and can be much brighter than the star itself at visible wavelengths (Hartigan et al. 1991). At longer wavelengths continuum excess from the veiling luminosity decreases, but thermal emission from hot dust in the circumstellar disk becomes an increasing and eventually dominant component of

the photospheric excess. Strom et al. (1989) have found excess emission as large as $\Delta K = 0.6$ mag above photospheric levels from broadband photometry of classical T Tauri stars. Either of these mechanisms may produce excess 2 μm continuum emission in the HL Tauri point source and thus affect the K magnitude estimated above. J. Carr has measured the veiling of HL Tau in the photospheric 2.3 μm CO band head absorptions and finds that 80% of the continuum emission at this wavelength derives from veiling (J. Carr, personal communication). This adjusts the photospheric magnitude corrected for reflection and veiling (but not extinction) to $K = 9.2$.

If this were the true photospheric K magnitude, a 4000 K blackbody could be extrapolated from this point to give predicted photospheric visual magnitudes for V, R, and I. These are $V = 12.1$, $R = 11.2$, and $I = 10.7$. Along with the observed limiting magnitudes at the stellar position, these determine extinctions of $A_V > 13.4$, $A_R > 12.8$, and $A_I > 12.2$ at the stellar position. Note that these are the extinctions toward the *unseen* point source. They are not applicable to analysis of the reflection nebula photometry, where the light takes a different path toward the observer. For these V, R, and I extinctions, standard reddening laws predict significant K-band extinctions exceeding 1.3, 1.7, and 2.1 mag, respectively. It is clear that the I-band limit provides the strongest constraint on the K-band extinction and thus on the total luminosity. Using this value, the corrected photospheric K magnitude would be <7.1, the expected $V < 10.0$, and the equivalent $A_V > 22$. Similar limits for A_V are derived by Beckwith & Birk (1995) from analysis of the near-infrared colors of the nebulosity. A 4000 K blackbody through $K < 7.1$ has a total luminosity of $>3.0\ L_\odot$ at HL Tau's distance of 140 pc; see Figure 4. This luminosity estimate must be considered uncertain by 30% because of the optical and infrared variability of HL Tau (Rydgren, Schmelz, & Zak 1984) and the lack of simultaneous photometry. It would be very valuable to have high resolution images and veiling measurements at other near-infrared wavelengths. This combination of data would allow the photospheric flux to be isolated from veiling and reflection contributions as done here for K band and would build up an actual spectral energy distribution for the star and the veiling.

We believe that $L > 3.0\ L_\odot$ is the best photospheric luminosity estimate currently available for HL Tau. The system luminosity, which includes both the photosphere and the optical veiling from accretion, will be significantly larger. A system luminosity of 6–7 $L_\odot$ is indicated by the geometric dilution induced by the reflection nebula on the luminosity estimates of previous workers. This value is reasonably close to the bolometric system luminosity of 5.6 $L_\odot$ derived by Cohen, Emerson, & Beichman (1989). The photosphere thus appears to contribute more than half the luminosity in the system. Pre–main-sequence evolutionary tracks run vertically in the region of the H-R diagram appropriate to HL Tauri (D'Antona & Mazzitelli 1994), and thus the new luminosity of 3 $L_\odot$ revises the theoretical age of the star down to only 10^5 yr.

HL Tau is thus significantly younger than is typical for classical T Tauri stars in Taurus-Auriga (ages $\approx 10^6$ yr; Strom et al. 1989; Beckwith et al. 1990). The large extinction found toward the star and the bright circumstellar reflection nebulosity are reminiscent of other embedded young stars such as L1551 IRS 5 and are hardly typical of T Tauri stars. Evidence for an infalling envelope in HL Tau has been derived from infrared spectral modeling and millimeter-wave kinematics (Calvet et al. 1994; Hayashi et al. 1993). These WFPC2 images, when combined with the other evidence, make clear that HL Tau is in an intermediate state of pre–main-sequence evolution between protostars and classical T Tauri stars.

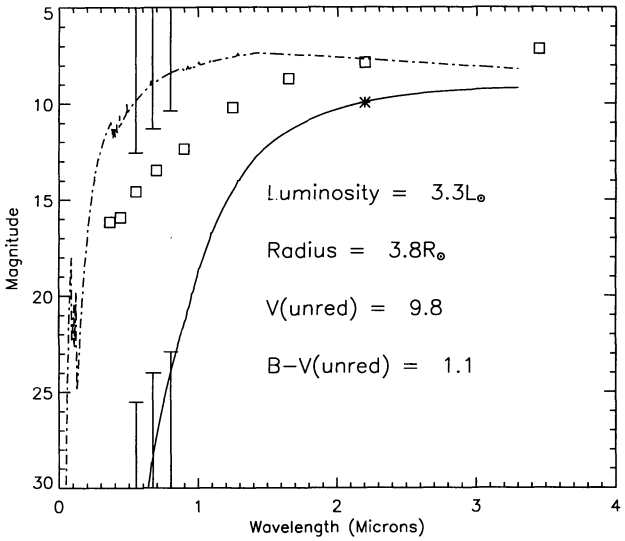

FIG. 4.—The spectral energy distribution for HL Tau. The photospheric K magnitude corrected for reflection, veiling, and extinction is 7.1 (indicated by the asterisk). The open squares represent observed ground-based magnitudes from Strom et al. (1989). Three bars at the top left represent WFPC2 photometry of the nebula; at the bottom left, three bars represent the WFPC2 upper limits to the stellar point source magnitude. The dotted line is an unreddened 4000 K blackbody; the solid line represents this blackbody reddened by $A_V = 22$ mag, which is the minimum extinction required to be consistent with the observed magnitude limits.

5. CONCLUSIONS

1. New WFPC2/*HST* observations of HL Tauri reveal that this object is actually a compact reflection nebula at optical wavelengths. There is no optically visible star to a limiting magnitude of $V = 25.5$; thus HL Tauri is deeply embedded in surrounding circumstellar matter.

2. The bright core of the reflection nebula has an unusual morphology which lacks symmetry about the outflow axis. The sharp southwest edge of the nebula defines a disk position angle of 145° within 50 AU of the star and shows that the diameter of the outflow cavity is comparable to the disk diameter (100 AU) where the two structures meet.

3. Previous determinations of the luminosity of HL Tauri are obsolete. The new value for the photospheric luminosity is $L > 3.0\ L_\odot$, or 3 times larger than previous estimates. This reduces the theoretical age of the system to just 10^5 yr. We estimate $A_V > 22$ mag toward the unseen point source.

4. The case of HL Tau suggests that other optically visible young stellar objects with large polarizations and infrared luminosity excesses (PV Cep, for example) may actually be seen via reflection. Interpretation of the spectral energy distributions for such "optically visible" sources may require revision, as suggested by Hamann & Persson (1992).

We wish to thank John Carr (Ohio State University) for providing us with a measurement of HL Tau's 2.3 μm continuum veiling. We also thank the referee for useful comments. This work was conducted at the Jet Propulsion Laboratory, California Institute of Technology, and at the Space Telescope Institute operated by AURA, under contracts with the National Aeronautics and Space Administration. K. R. S. acknowledges support from the NASA Origins of Solar Systems Research Program.

REFERENCES

Adams, F. C., Emerson, J. P., & Fuller, G. A. 1990, ApJ, 357, 606
Adams, F. C., Lada, C. J., & Shu, F. H. 1988, ApJ, 326, 865
Basri, G., & Batalha, C. 1990, ApJ, 363, 654
Bastien, P. 1982, A&AS, 48, 153
Beckwith, S. V. W., & Birk, C. C. 1995, ApJ, submitted
Beckwith, S. V. W., Sargent, A. I., Chini, R. S., & Güsten, R. 1990, AJ, 99, 924
Beckwith, S. V. W., Sargent, A. I., Koresko, C. D., & Weintraub, D. A. 1989, ApJ, 343, 393
Beckwith, S. V. W., Zuckerman, B., Skrutskie, M. F., & Dyck, H. M. 1984, ApJ, 287, 793
Boss, A. P. 1987, ApJ, 316, 721
Burrows, C. J., ed. 1994, Hubble Space Telescope Wide Field and Planetary Camera 2 Instrument Handbook, Version 2.0 (Baltimore: Space Telescope Science Institute)
Calvet, N., Hartmann, L., Kenyon, S. J., & Whitney, B. A. 1994, ApJ, 434
Cohen, M. 1983, ApJ, 270, L69
Cohen, M., Emerson, J. P., & Beichman, C. A. 1989, ApJ, 339, 455
Cohen, M., & Kuhi, L. V. 1979, ApJ, 41, 743
Cohen, M., & Witteborn, F. C. 1985, ApJ, 294, 345
D'Antona, F., & Mazzitelli, I. 1994, ApJ, 90, 467
Gledhill, T. M., & Scarrott, S. M. 1989, MNRAS, 236, 139
Grasdalen, G. L., Sloan, G., Stout, M., Strom, S. E., & Welty, A. D. 1989, ApJ, 339, L37
Haas, M., Leinert, C., & Zinnecker, H. 1990, A&A, 230, L1
Hamann, F., & Persson, S. E. 1992, ApJ, 394, 628
Hartigan, P., Kenyon, S. J., Hartmann, L., Strom, S. E., & Edwards, S. 1991, ApJ, 382, 617
Hayashi, M., Ohashi, N., & Miyama, S. M. 1993, ApJ, 418, L71
Herbig, G. H., & Bell, K. R. 1988, Lick. Obs. Bull., 1111, 1
Holtzman, J. A., et al. 1995, PASP, 107, 156
Lay, O. P., Carlstrom, J. E., Hills, R. E., & Phillips, T. G. 1994, ApJ, 434, L75
Montgomery, K. A., Marschall, L. A., & Janes, K. A. 1993, AJ, 106, 181
Mundt, R., Ray, T. P., Bührke, T., Raga, A. C., & Solf, J. 1990, A&A, 232, 37
Reipurth, B. 1989, A&A, 220, 249
Rodríguez, L. F., Cantó, J., Torrelles, J. M., Gómez, J. F., Anglada, G., & Ho, P. T. P. 1994, ApJ, 427, L103
Rydgren, A. E., Schmelz, J. T., & Zak, D. S. 1984, Pub. USNO, 25, 1
Sargent, A. I. 1989, in The Formation and Evolution of Planetary Systems, ed. H. A. Weaver, & L. Danly (New York: Cambridge Univ. Press), 111
Sargent, A. I., & Beckwith, S. V. W. 1991, ApJ, 382, L31
Sargent, A. I., & Koerner, D. W. 1995, in preparation
Solf, J., & Böhm, K. H. ApJ, 375, 618
Strom, K. M., Strom, S. E., Edwards, S., Cabrit, S., & Skrutskie, M. F. 1989, AJ 97, 1451
Strom, K. M., Strom, S. E., Wolff, S. C., Morgan, J., & Wenz, M. 1986, ApJS, 62, 39
Trauger, J. T., et al. 1994, ApJ, 435, L3
Whitney, B. A., & Hartmann, L. 1992, ApJ, 395, 529
Whittet, D. C. B., Bode, M. F., Longmore, A. J., Baines, D. W. T., & Evans, A. 1983, Nature, 303, 218